Review Article

Bone marrow magnetic resonance imaging (MRI): morphological and functional features from reconversion to infiltration

Cristina Vilanova[1]^, Teodoro Martín-Noguerol[2]^, Roberto García-Figueiras[3], Sandra Baleato-González[3], Joan C. Vilanova[4]^

[1]Department of Orthopaedic Surgery, Hospital Germans Trias i Pujol, Barcelona, Spain; [2]MRI Unit, Radiology Department, HT Medica, Jaén, Spain; [3]Department of Radiology, Hospital Clínico Universitario de Santiago de Compostela, Galicia, Spain; [4]Department of Radiology, Clínica Girona, Institute of Diagnostic Imaging (IDI) Girona, University of Girona, Girona, Spain

Contributions: (I) Conception and design: JC Vilanova; (II) Administrative support: C Vilanova, JC Vilanova; (III) Provision of study materials or patients: None; (IV) Collection and assembly of data: None; (V) Data analysis and interpretation: None; (VI) Manuscript writing: All authors; (VII) Final approval of manuscript: All authors.

Correspondence to: Joan C. Vilanova, MD, PhD. Department of Radiology, Clínica Girona, Institute of Diagnostic Imaging (IDI) Girona, University of Girona, C. Barcelona 206, 17005 Girona, Spain. Email: kvilanova@comg.cat.

Abstract: Bone marrow is a dynamic organ with variable composition in relation to age or pathophysiological changes. Magnetic resonance imaging (MRI) is the technique of choice to assess the different components of the bone marrow based on the different information provided by the different characteristics of the MRI sequences. This article provides an overview of the MRI appearances of normal and abnormal bone marrow. We review the MRI features of normal developmental red marrow- to yellow-conversion, reconversion and physiologic conditions. We review the key imaging techniques used in assessing bone marrow pathology in MRI, including T1-weighted, T2-weighted, Dixon chemical shift imaging and diffusion-weighted imaging, as well as dynamic contrast-enhanced (DCE) MRI. It is discussed the bone marrow characteristics in the different morphological and functional MRI sequences from the normal or abnormal conditions such as; infiltration (metastases), proliferation [multiple myeloma (MM)], vascular edema/necrosis and postreatment changes. We show the different MRI features to differentiate physiological processes from pathological processes in order to provide effective diagnoses, as well as to evaluate the optimal therapeutic monitoring assessment. Insights from recent advancements in imaging technology and emerging MRI techniques are also discussed, providing a comprehensive overview of bone marrow MRI and its clinical implications. This review provides a useful tool for radiologist to decide normal or abnormal findings from the analysis of bone marrow MRI; in order to manage and take decisions that will depend on the imaging findings. The optimal analysis of bone marrow MRI requires knowledge of the physiology of the bone marrow to interpret properly the pathology and avoid diagnostic errors.

Keywords: Bone marrow; magnetic resonance imaging (MRI); red and yellow bone marrow; metastases

Submitted Nov 25, 2023. Accepted for publication Mar 12, 2024. Published online Apr 08, 2024.
doi: 10.21037/qims-23-1678
View this article at: https://dx.doi.org/10.21037/qims-23-1678

^ ORCID: Cristina Vilanova, 0009-0008-6909-390X; Teodoro Martín-Noguerol, 0000-0001-7200-5028; Joan C. Vilanova, 0000-0003-2148-6751.

Introduction

Bone marrow is a dynamic organ formed by a trabecular bone tissue and a cellular tissue in continuous change since birth. Its composition is variable in relation to age or pathophysiological changes. For a long time, techniques such as plain radiography, computed tomography (CT) and bone scintigraphy have been used to assess cortical and trabecular bone (1), but these techniques are not sensitive to changes in the bone marrow composition. Magnetic resonance imaging (MRI) is the technique of choice to assess the different components of the bone marrow based on the different information provided by the different characteristics of the MRI sequences. MRI is an effective technique for assessing and differentiating physiological processes from pathological processes, especially in the management of infiltrative pathology, especially metastases (2). This differentiation is a challenge for radiologist to decide normal or abnormal findings from the analysis of bone marrow MRI; in order to manage and take decisions that will depend on the imaging findings. The optimal analysis of bone marrow MRI requires knowledge of the physiology of the bone marrow to interpret properly the pathology and avoid diagnostic errors.

We provide an overview of the MRI appearances of normal and abnormal bone marrow. It is discussed the bone marrow characteristics in the different morphological and functional MRI sequences from the normal or abnormal conditions such as; infiltration (metastases), proliferation [multiple myeloma (MM)], vascular edema and postreatment changes.

Bone marrow

Bone marrow is a gelatinous tissue consisting of hematopoietic stem cells, adipose cells, and stroma contained within the medullary space, made up of a bony trabecular network, vessels and vascular sinuses, nerves, reticulum cells, and lymphoid tissue. The composition is variable in relation not only to individual physiological conditions but also depending on age. Normal bone marrow is composed of different proportions of red marrow (hematopoietic bone marrow) and yellow marrow (inactive hematopoietic marrow), with different contents in relation to the proportion of hematopoietic cells, water and fat. Red marrow contains 40% fat cells, 40% water, 20% hematopoietic cells, while yellow bone marrow is made up of 80% fat cells, 15% water, and 5% hematopoietic cells (3). After childhood, red bone marrow is replaced by yellow marrow through a process of progressive conversion from the periphery (appendicular skeleton) to the center (axial skeleton) and from the distal epiphyses to the diaphyses to the proximal metaphyses of the long bones. In long bones, it is common to observe remains of subchondral red marrow, especially in the head of the humerus and femur. In adults, the red marrow is found mainly in the metaphysis of the appendicular and subcortical skeleton of the vertebral platform (the metaphyseal equivalent) and pelvis, due to its own vascularization (4).

The reconversion of yellow bone marrow to red occurs in certain circumstances due to increased demand for hematopoiesis. This process occurs in the opposite direction to the conversion, starting in the axial skeleton to the extremities. The different causes that can cause bone marrow reconversion are detailed in *Table 1*.

Bone marrow MRI

MRI is the technique of choice to manage bone marrow and especially in the spine (5,6), due to its ability to identify the physiology and changes of the bone marrow based on the different characteristics provided by the different sequences used (*Figure 1*).

MRI sequences

It is essential to know the normal appearance of the bone marrow based on the different conventional sequences [spin echo T1, T2 with fat suppression-short tau inversion recovery (STIR), chemical shift-phase/out of phase, diffusion-weighted imaging (DWI) or dynamic contrast-enhanced (DCE) MRI] to differentiate normal, variants and physiological changes of the yellow and red marrow. *Table 2* describes the signal patterns based on the different sequences and the findings in relation to the yellow and red marrow and the lytic or blastic infiltrative processes (7).

The essential morphological sequences for bone marrow analysis are T1 spin echo and STIR or T2 fat suppression. Fat has a shorter T1 than water and the highest signal. Thus fatty marrow exhibits a high signal intensity (SI) in T1 (8). A 180-degree inversion pulse is used initially for a STIR sequence. The inversion time is chosen to cancel the signal of fat. The main drawback of the STIR sequence is that it cancels every signal identical to fat (e.g., blood in hematoma or contrast-enhanced tissue). To overcome this

Table 1 Causes of reconversion from yellow marrow to red marrow

Bone marrow infiltration (metastasis, hematological diseases)
Severe anemia
Chronic heart failure
Hematopoietic stimulating factors
Extensive irradiation (reconversion in non-irradiated marrow)
Long distance runners
Residence at altitude
Excessive smoking
Obesity

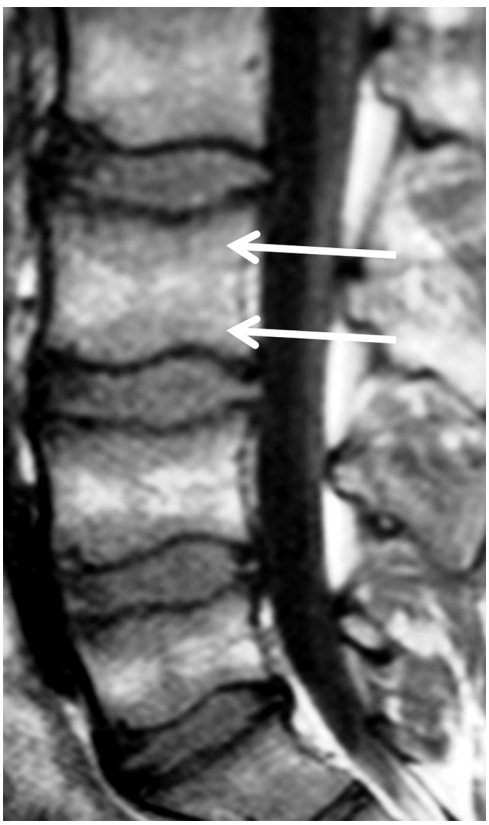

Figure 1 Bone marrow reconversion. A 37-year-old male long-distance runner. Sagittal FSE T1 showing reconversion of the yellow marrow to red marrow in the platform region, vertebral epiphysis (arrows). FSE, fast spin echo.

drawback it can be used T2 fat suppression. The difference between fat and water proton frequency is also used for fat presaturation. A saturation pulse with a narrow band at the exact fat frequency is used before the usual pulse. A very homogeneous magnetic field is required; therefore this sequence, T2 fat suppression is not effective on every unit but more specific (9).

The ease in detecting low SI of infiltrative lesions of the bone marrow in T1 surrounded by the normal high signal of fatty marrow explains the usefulness of the T1 sequence to detect bone marrow lesions. In general, diffuse lower signal involvement of the bone marrow compared to iso or higher SI of the disc in T1 is usually pathological with a reliability of 98% (1). On the other hand, the presence of high signal foci (fat) in the center of a bone marrow lesion on T1 (bull's eye sign) has a specificity of 99.5% and sensitivity of 98% for benign lesion (10) (*Figure 2*). In T2 sequences (fat suppression or STIR) it is useful to identify a perilesional hyperintense ring (halo sign) (*Figure 3*) as a specific sign (99.5%) of a metastatic infiltrative process (10).

Currently, it is useful to include DWI sequence and the apparent diffusion coefficient (ADC) for the assessment of bone marrow in infiltrative processes. For the analysis of the bone marrow with DWI sequence, it is necessary to consider the presence of fatty marrow content within the analysis of T1 sequence and fat suppression in T2 or STIR. The increase in adipose content within the bone marrow with age shows a negative correlation with ADC values, therefore the higher the fatty content, the more negative the ADC value is (*Table 2*). ADC values shows a negative correlation with the cellularity of the bone marrow, although paradoxically, the ADC of the hypocellular yellow marrow is lower than the ADC of normal normocellular marrow of adults and the hypercellular marrow of children (11). At a microscopic level, yellow marrow adipocytes show greater restriction to water diffusion than normal hematopoietic cells. Special caution should be taken when using DWI in the evaluation of bone pathology in children, since areas of higher signal at high b values (b>500 s/mm^2) are common in the pelvis and lumbar spine.

DCE-MRI is an MRI sequence that enables to dynamically assess the vascularization of biological tissues by real-time monitoring of contrast, gadolinium, passing through the capillary network. DCE-MRI sequences typically use a T1-weighted spoiled gradient echo repeated several times after intravenous contrast agent administration, offering high temporal and intermediate spatial resolution. DCE sequence is less useful to evaluate bone marrow, as both normal red marrow and various diseases (infection, inflammation, and tumor) can enhance (12). The degree of normal marrow enhancement depends on the distribution

Table 2 Bone marrow signal in the different processes related to the MRI sequence

Sequence	Signal (related to vertebral disc)			
	Yellow marrow	Red marrow	Lytic	Blastic
T1	↑	=	↓	↓
T2 fat suppress (STIR)	↓	=↑	↑	↓
In phase	↑	=	=	↓
Out phase	↓	↓	=↑	↓
Diffusion	↓	=	↑	↓
ADC (mm^2/s)	$<0.4\times10^{-3}$	$(0.4–0.6)\times10^{-3}$	$(0.6–0.9)\times10^{-3}$	~0
Contrast (T1 fat sup)	↓	=	↑	↓

MRI, magnetic resonance imaging; STIR, short tau inversion recovery; ADC, apparent diffusion coefficient.

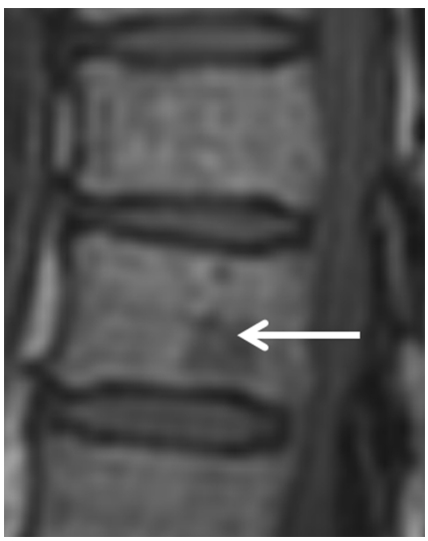

Figure 2 Sagittal T1 of the spine showing central high signal in a hypointense focal area, indicative of fat, in relation to the rest of normal red marrow (arrow), "bull's eye" sign.

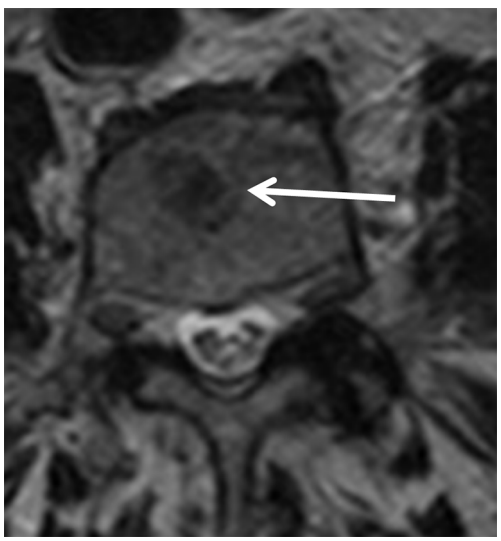

Figure 3 Axial T2 of the lumbar spine showing nodular lesion with a more hyperintense peripheral halo in the vertebral body (arrow) due to edema, indicative of metastasis.

and volume of red marrow. Therefore, in infants and young children with almost entirely hematopoietic marrow, contrast enhanced images are even less sensitive in detection of subtle marrow disease.

The inclusion of in-phase/out-of-phase Dixon chemical shift imaging sequence is very useful to evaluate the bone marrow (13). Dixon techniques can be used to acquire several echoes in the same sequence and combine them through mathematical postprocessing of data to obtain not only in-phase or opposed-phase images but also a fat-only image (by subtracting the SI of the in-phase image from that of the out-of-phase image) and a water-only image (by adding both signal intensities). Thus, the Dixon technique may be considered a hybrid sequence where four sets of images are obtained from only one acquisition (*Figure 4*). The fat-only images offer the potential for fat quantification, and the water-only images are excellent for postcontrast T1-weighted imaging. The in-phase and out-of-phase acquisition technique provides information on microscopic fat, and makes it especially useful in differentiating normal bone marrow with abundant fat from a pathological condition that can replace the normal

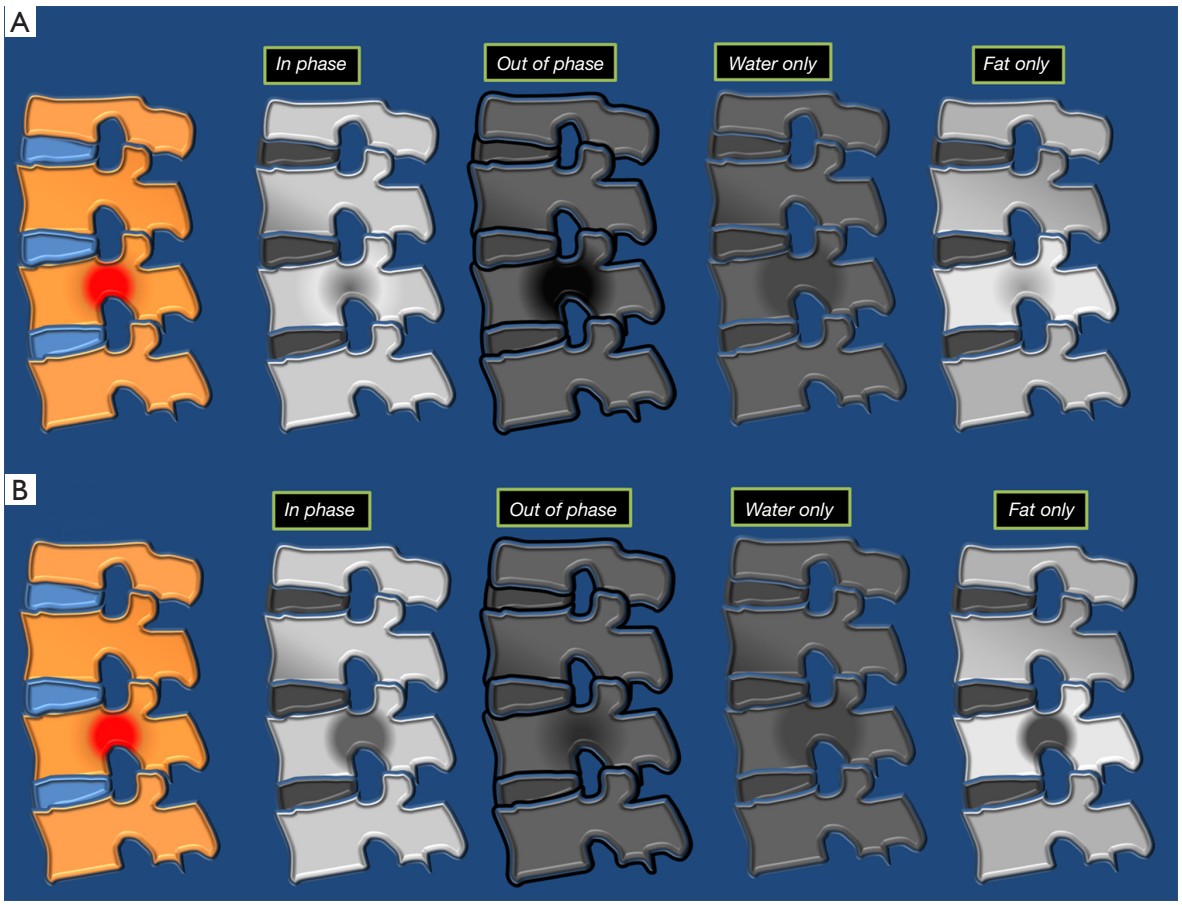

Figure 4 Chemical shift imaging and Dixon acquisition. Drawing shows the 4 images after Dixon acquisition. The signal intensities of the in-phase and opposed-phase images are added or subtracted to obtain a water-only or fat-only set of images, respectively. (A) A hypointense area on in-phase image that becomes with significantly lower signal on out-phase images and not as low in fat only images indicates high amount of microscopic fat consistent with a benign lesion. (B) A hypointense area on in-phase image that does not become with significantly lower signal on out-phase images and with lower signal in fat only images indicates low amount of microscopic fat consistent with a malignant lesion.

bone marrow. On the other hand, when fat is not replaced (such as edema or red marrow mixed with yellow marrow), there will be a decrease in SI in the opposite phase image compared to the in-phase image (*Figure 4*). The ratio of the SI of the bone marrow in the opposite phase image to that of the phase image can be calculated by placing a region of interest (ROI). It has been shown that SI ratio >0.8 is suggestive of a malignant process and SI <0.8 is suggestive of a benign process (14). Likewise, the percentage of signal loss between the in-phase and out-of-phase image can be used. A signal loss of >20% between the in-phase and out-of-phase images indicates high fatty content, indicative of benign process; while a signal loss <20% indicates low fatty content and may indicate an infiltrative process (14).

Conversion-reconversion: a guide to MRI interpretation

Different causes that can cause bone marrow reconversion are detailed in *Table 1*. Persistent red bone marrow is frequently found in routine MRI exams, and can give rise to unusual red marrow patterns that could be misinterpreted as a malignant process, if not carefully analyzed. Widespread, diffuse red marrow may be difficult to differentiate from a diffuse hematologic malignancy (15).

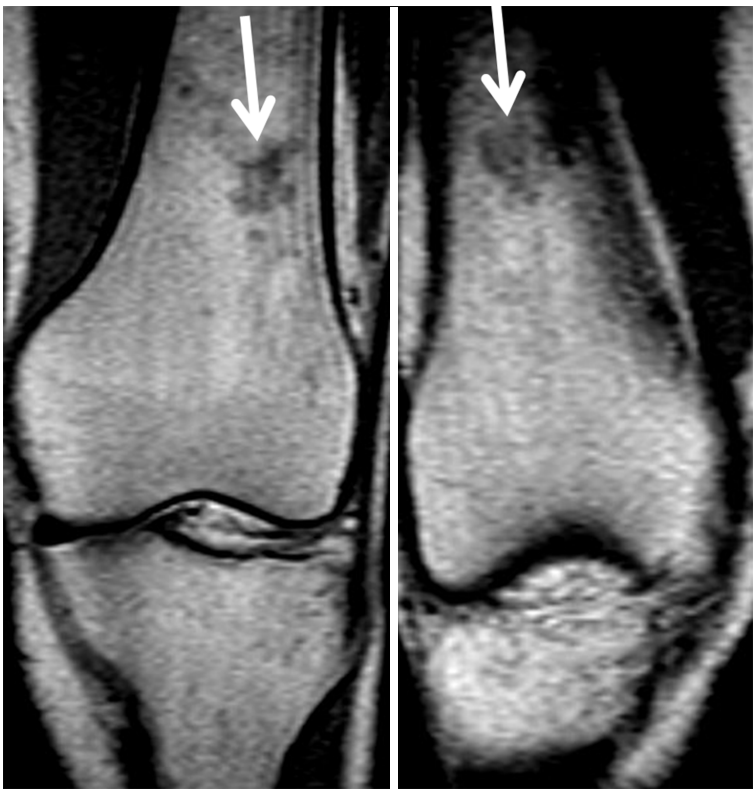

Figure 5 Coronal image in out-of-phase T1 sequence of both knees showing focal hyposignal in the bone marrow with a symmetrical distribution in the distal diaphysis of the femur (arrows) indicative of red marrow remains.

The radiologist must recognize and understand the physiological and pathological changes of the bone marrow in relation to age, variants, normal patterns and identify pathological processes in relation to the different causes. Correlation of image findings with clinical parameters will be essential for correct interpretation (16).

T1 sequence should be the first to be analyzed, in which any hypointense area within the normal hypersignal of the yellow marrow will be most easily detected. The presence of low signal in T1 of the bone marrow may correspond to a pathological process or persistent red marrow (15). Red marrow shows higher signal than the intervertebral disc or muscle in T1, than a pathological process such as metastasis; making it an effective sign to differentiate normal bone marrow from pathological bone marrow (17). Another useful parameter to differentiate red bone marrow from pathological process is the symmetry of normal red bone marrow in both extremities in the same patient. Thus, it may be useful in cases of doubtful images in an extremity to perform a T1 sequence of the contralateral extremity to observe the same distribution of normal red bone marrow (*Figure 5*).

Bone marrow pathology

Infiltration: *bone metastases*

Bone is the most frequent location of metastases after the liver and lungs. Metastases are the most common cause of bone tumors, representing 25% of cases. Furthermore, the spine represents the most frequent location of skeletal metastases. Precisely, the most frequent location of metastases is the axial skeleton and proximal end of the long bones; due to the presence of persistence red marrow (18). Malignant cells can spread to the spinal column by various mechanisms: through the arterial system, through venous drainage, through cerebrospinal fluid, or by direct extension. The main route of dissemination for metastases in the spine is through the paravertebral venous plexus of Batson, consisting of a complex valveless plexiform network of paraspinal veins; thus avoiding the lung filter. The increased presence of red marrow in the spine provides more vascularization, which

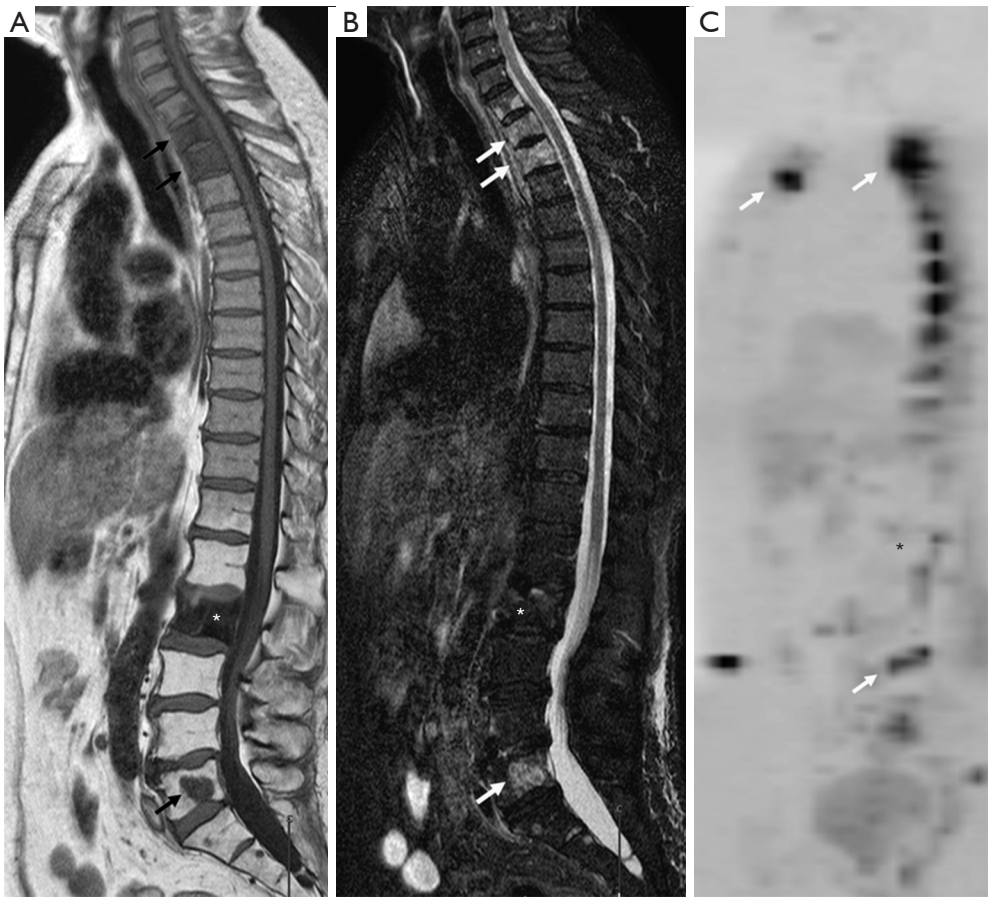

Figure 6 Osteolytic and osteoblastic vertebral metastases from prostate carcinoma. Osteolytic metastases with diffusion restriction are observed at the upper dorsal, L5 and sternal levels (arrows) and an osteoblastic metastasis in L2 (asterisk), which does not present diffusion restriction and is markedly hypointense on T1 (A) and STIR (B). In the diffusion sequence, no involvement of the blast vertebra is observed (asterisk) (C). STIR, short tau inversion recovery.

explains the increased frequency of metastases of the spine; as well as the more frequent involvement of the pedicle, unlike MM (19).

During metastatic cell proliferation in the bone, two simultaneous or sequential phenomena occur: bone proliferation and destruction influenced by the activation-stimulation of osteoblasts and osteoclasts, providing the phenomenon of resorption or production of bone matrix; causing osteoblastic, osteolytic or mixed metastasis based on the higher or lesser activation of the different osteoclastic or osteoblastic stimulating factors (20). Primary neoplastic cells stimulate the different blastic or lytic activation factors differently based on the primary tumor, but heterogeneously in the different bone regions (21). In this sense, metastases tend to have a more or less lytic or blastic appearance in relation to the primary tumor, being mostly of a mixed appearance in the same patient (*Figure 6*). In addition, there is the influence of angiogenic factors that explain vascularized metastases with an expansive appearance on imaging, as it is the case in kidney cancer.

MRI detection of metastases

Diagnosis of bone metastases is crucial in order to determine the prognosis and to optimize therapy. As described, metastatic bone lesions can be osteolytic or osteoblastic. MRI is shown to be the most reliable technique for its detection precisely because of its effectiveness in evaluating the bone marrow and allows the evaluation of both blastic and lytic lesions. Lytic metastases typically show low signal in T1, and high signal on STIR or fat suppression T2 (*Table 2*). Osteoblastic metastases appear as hypointense areas in the

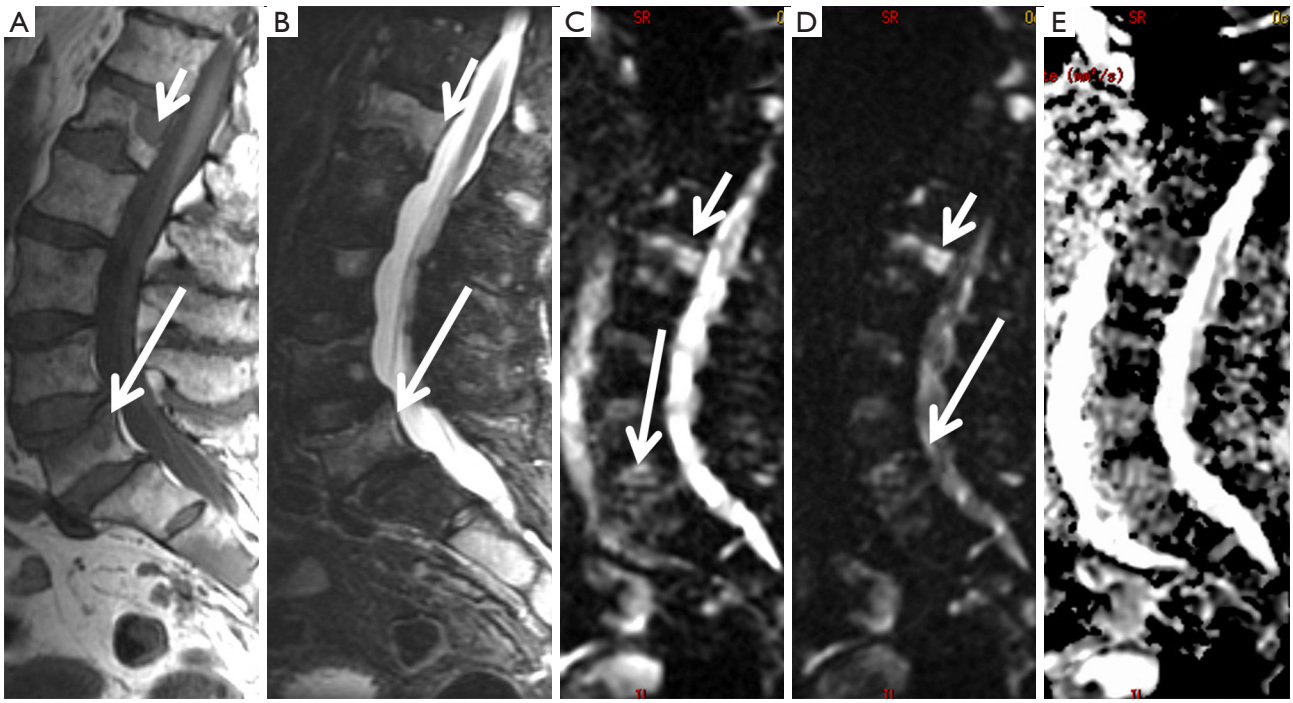

Figure 7 Benign and malignant edema on the ADC map. Lumbar MRI in a patient with known bone metastasis from breast cancer, currently presenting with acute low back pain. (A) Sagittal in FSE T1 showing multiple focal lesions, especially in L1 (short arrow) and diffuse edema in L5 (long arrow). (B) The corresponding sagittal STIR shows a more diffuse edema at both levels that is difficult to differentiate whether infiltrative or non-infiltrative. (C) Sagittal diffusion at b=0 mm^2/s and (D) at b=800 mm^2/s showing the persistence of hypersignal from the lesion at the level of L1 (short arrow) and lower signal at L5 (long arrow). (E) The sagittal section on the ADC map confirms the hyposignal in L1 (short arrow) with an ADC value of 0.7×10^{-3} mm^2/s and hypersignal in L5 with an ADC value of 1.6×10^{-3} mm^2/s. The lesion in L1 is due to a metastasis and in L5 due to an insufficiency fracture, where the sagittal FSE T1 image (A) shows a subcortical horizontal line (arrow), which justifies the current symptoms. ADC, apparent diffusion coefficient; MRI, magnetic resonance imaging; FSE, fast spin echo; STIR, short tau inversion recovery.

different sequences, especially in the diffusion sequence due to their low water content. In any case, the presence of mixed metastases is common, so in fat suppression/STIR sequences they can be seen with high signal in relation to the proportion of blastic or lytic component (*Figure 6*).

The analysis of metastases requires combined morphological and functional assessment. In this sense, it is always necessary to perform the analysis of the DWI sequence combined with the other morphological sequences T1, T2, fat suppression or STIR. Fatty bone marrow shows a very low ADC value. In vertebral fractures, the influence of fat decreases, thus malignant fractures show lower ADC values (between 0.7×10^{-3} and 1×10^{-3} mm^2/s) than osteoporotic or insufficiency fractures [$(1–2)\times10^3$ mm^2/s] (22) (*Figure 7*). There is overlap in ADC values between malignant processes affecting the bone marrow and infectious spondylitis, which generally shows low ADC values.

It is necessary to use and combine all the morphological and functional information from the different MRI sequences for correct interpretation and to differentiate a metastatic lesion from a benign fracture. *Table 3* details the combined criteria for a correct analysis of metastatic lesions. In inconclusive cases it will be necessary to either perform an image control or a biopsy.

The management of the different imaging techniques for the detection of bone metastases will be influenced by different factors: primary tumor, availability of the technique, clinical history and the decision agreed upon by the different oncological committees.

Proliferation: MM

MM is a malignant disease of plasma cells, characterized by infiltration of the bone marrow with clonal plasma

Table 3 Magnetic resonance imaging features of benign versus malignant spine lesions

MRI feature	Benign	Malignant
Fracture line	Clearly distinct	Indistinct
Bone marrow pattern	Normal, preserved	Focal, geographic, diffuse
Morphology	Horizontal bandlike, retropulsed bone fragment, posterior cortex of vertebral body has acute angle	Rounded, diffuse, or irregular; pedicle involved, paravertebral and/or epidural mass, posterior cortex of vertebral body is smooth, convex toward canal
T2WI	Intact posterior body wall	Disrupted posterior body wall
STIR	Lower signal intensity ratio	Higher signal intensity ratio
Dynamic intravenous contrast	No or slow enhancement	Rapid wash-in and early washout
Diffusion-weighted	Higher ADC	Lower ADC
Dual-phase chemical shift (in/out of phase)	Low signal intensity ratio	High signal intensity ratio
	In phase: low SI	In phase: low SI
	Out of phase: low SI	Out of phase: high SI

MRI, magnetic resonance imaging; T2WI, T2-weighted imaging; STIR, short tau inversion recovery; ADC, apparent diffusion coefficient; SI, signal intensity.

cells; production of monoclonal immunoglobulin (paraprotein), organ damage, lytic bone lesions, renal failure, hypercalcemia and anemia. The pathophysiological mechanism of MM consists of the stimulation of osteoclasts and the inhibition of osteoblasts by myelomatous cells, which explains the lytic image of MM in the different imaging techniques (23). MM is part of the plasma cell diseases characterized by the production of a paraprotein; which include symptomatic MM, latent MM (asymptomatic), monoclonal gammopathy of undetermined significance (MGUS), solitary plasmacytoma, systemic amyloidosis, POEMS syndrome and Waldestrom macroglobulinemia. Both latent MM and MGUS are considered precursors to symptomatic MM. Plasmacytoma is the focal variant of MM. MM can be the cause of primary amyloidosis. The diagnosis of MM includes: >10% plasma cells in bone marrow, diagnosis of plasmacytoma in biopsy, detection of monoclonal protein in serum or urine and the presence of organic lesion (hypercalcemia, renal failure, anemia or lytic bone lesions) (24).

MRI detection of MM

Currently, imaging techniques play a relevant role in the management of MM. International guidelines recommend the use of whole body techniques; low-dose CT, whole-body MRI or PET-CT in the diagnosis and treatment of MM, replacing skeletal survey (24). The selection of one or another technique depends on the clinical situation and their different availability. MRI is the technique of choice in the analysis to detect lesions in the bone marrow of MM. A specific guide has been developed for the acquisition, interpretation and monitoring of MM in whole-body MRI called MY-RADS (25).

Three patterns of infiltration have been described in MM (26): focal, mottled or variegated ("salt and pepper") and diffuse; although the presence of a mixed, combined pattern is common; diffuse-multifocal (*Figure 8*). There is prognostic value in the diffuse pattern as it shows shorter survival time in MM. Likewise, the diffuse pattern tends to progress more rapidly than those with the mottled pattern. Precisely the usefulness of MRI is to be able to identify patients at highest risk based on MRI patterns and prevent complications. At the same time, MRI allows us to assess the evolution of the lesions.

MRI is useful in the management of plasmacytoma, MGUS, and latent MM to rule out bone lesions and exclude MM. MRI allows us to evaluate subgroups of patients who have a high risk of progression to MM disease, especially plasmacytoma. Multidetector CT is the alternative technique to bone serial in assessing the risk of fractures and loss of bone mass; together with the clinical-analytical data for the control of this subgroup of patients.

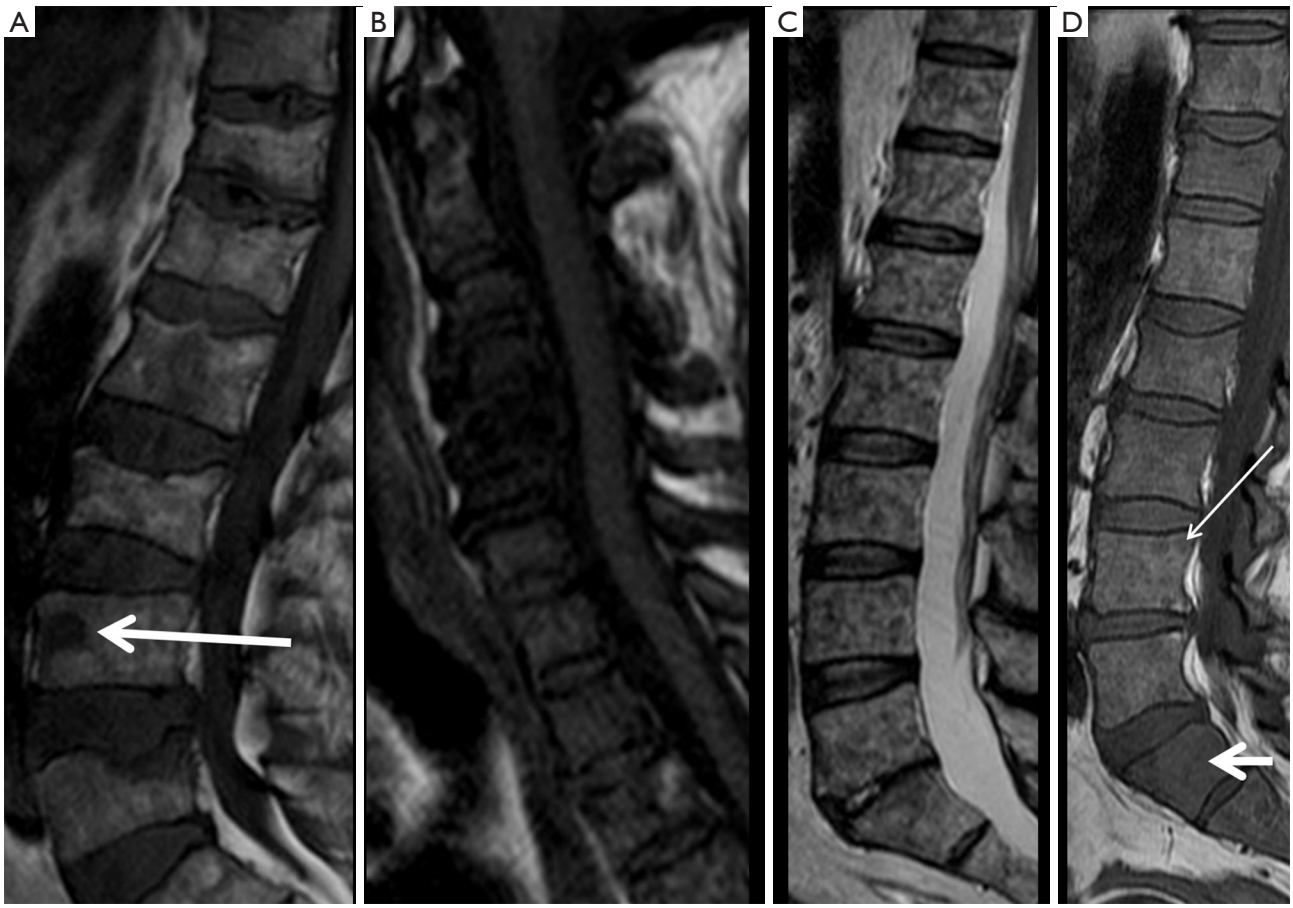

Figure 8 MRI patterns of multiple myeloma. (A) Sagittal FSE T1 showing nodular lesion in L4 (arrow) in relation to focal pattern, (B) sagittal FSE T1 showing diffuse infiltration of the bone marrow in the cervical vertebral bodies in relation to diffuse pattern, with superimposed osteoarthritis from C3 to C6, (C) sagittal on FSE T1 showing mottled, variegated or salt and pepper pattern; represented by diffuse micronodular lesions in the bone marrow and (D) sagittal in FSE T1 showing micronodular pattern in the vertebral bodies of the lumbar spine, similar to that observed in L4 (long date) together with diffuse infiltration of S1 (short arrow); in relation to combined-mixed pattern. MRI, magnetic resonance imaging; FSE, fast spin echo.

Vascularization: *edema*

The term bone marrow edema translates an increase in the inflammatory component and fibrosis, rather than the presence of an increase in the aqueous component as the edema terminology generally seems to indicate. On T1, bone marrow manifests with moderately low SI (higher than that of muscle or intervertebral discs) with a wide and poorly defined zone of transition to normal marrow. On T2, there is an increase in SI, more obvious on STIR or fat suppression T2. On T1 after contrast administration, the abnormal marrow edema enhances homogeneously. There should be no sharp or curvilinear interfaces of abnormal to normal bone marrow suggestive of an underlying abnormality, such as a bone tumor. The most important task when a bone marrow edema pattern is observed on MR images is to determine whether ist is transient (reversible), related to a self-limiting disorder, or associated with an irreversible, more serious pathology. The presence of edema without other adjacent signs is usually a reversible process depending on the clinical context and the presence or absence of a traumatic history (1). The differential diagnosis of bone marrow edema is very broad, but in the absence of trauma and without a relevant clinical context, it includes the so-called bone marrow edema syndromes. Some more relevant entities include transient edema (osteoporosis), migratory regional edema (osteoporosis), and complex regional pain syndrome (reflex sympathetic dystrophy) (4).

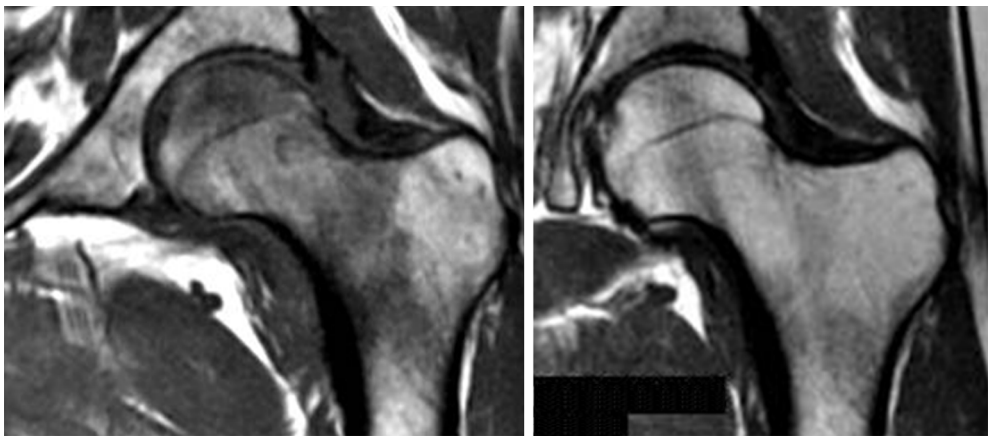

Figure 9 Transient edema (transient osteoporosis). Coronal T1 image of a pregnant woman with diffuse edema of the left femoral head and neck with complete resolution 3 months after unloading measurements (right image).

All of these syndromes show diffuse bone edema without chondral or subchondral lesions. The differential diagnosis of the different entities is based on clinical history, age, gender and symptoms. Quantitative MRI can be used to evaluate bone marrow changes such as the influence of high altitudes with increasing age and under the influence of long-term chronic hypoxia (27).

Transient edema (transient osteoporosis) generally affects the femoral head and is frequently described in pregnant patients (*Figure 9*). Transient migratory edema is an entity with no known etiology that can affect the hip, knee and tarsus, with a long-lasting clinical course and bilateral distribution; thus making the diagnosis difficult. Complex regional pain syndrome usually appears after trauma, with pain symptoms higher than expected in relation to the trauma. Nowadays there is controversy in considering transient edema and transient migratory edema as precursors or risk in subchondral fractures or in evolution to spontaneous osteonecrosis as occurs in the knee. It has been shown useful to use quantitative MR sequences to analyze the bone marrow and detect dysbaric change in the femoral heads of divers with hip pain as early signs to prevent osteonecrosis (28).

Therapeutic monitoring

Therapeutic monitoring using only morphological techniques is non effective because precisely sclerosis changes in response to treatment will not show the microscopic changes in T1 MRI sequences, as they can show similar findings before and after treatment (*Figure 10*). The use of RECIST or Anderson criteria has been shown to be ineffective, since they cannot measure pathophysiological aspects of the response in the morphological image of the metastases. Its assessment with functional sequences such as diffusion MRI is necessary and effective (*Figure 10*). A response criteria used in MRI is the presence of fatty marrow surrounding the lesion, a halo sign on T1 (29), in addition to being able to use the DWI sequence. In prostate cancer, a decrease in prostate-specific antigen (PSA) levels corresponds to an increase in the mean ADC. The evaluation of the response to treatment can be carried out using a qualitative and/or quantitative method. Effective treatment of a malignant lesion in the bone marrow shows increased ADC values due to increased water diffusion secondary to cell death. Normal bone marrow also shows fatty atrophy secondary to radiotherapy, which decreases its signal in the diffusion sequence with high b values.

Currently, clinical guidelines are including the standardized whole body MRI interpretation guides for therapeutic monitoring of bone metastases (MET-RADS) (30) and multiple myeloma (MY-RADS) (25).

Interpretation of signal changes in the bone marrow after effective treatment is complex due to its variability and generally patchy appearance. In this sense, the integration and analysis of all morphological and functional MRI sequences is essential for a correct assessment of the bone marrow, together with the clinical information.

It is useful to report MRI of bone marrow follow up after therapy using structured reports, in order to avoid ambiguity and making easier its comparison (31).

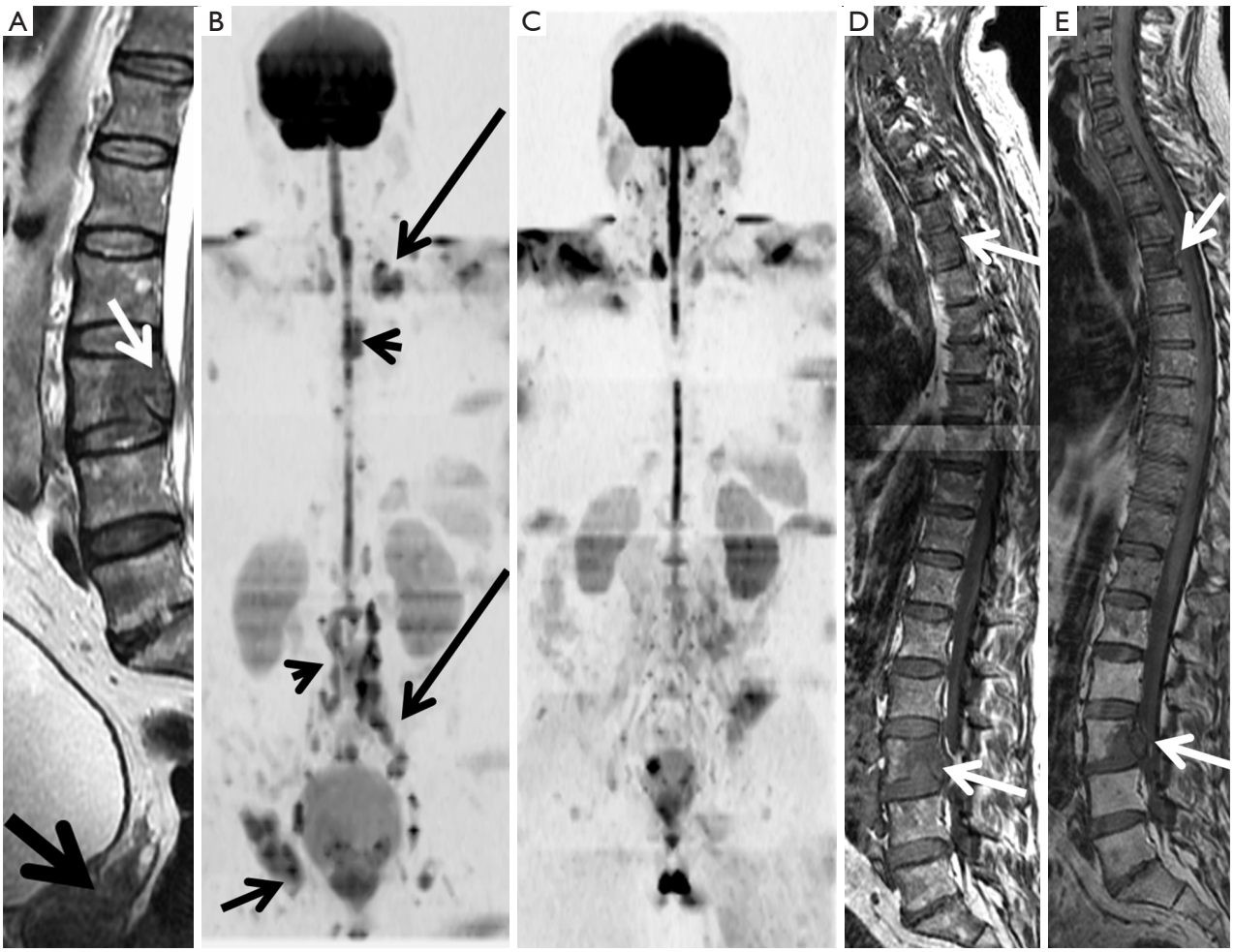

Figure 10 Sixty-one-year-old man with acute low back pain. (A) Detection of lumbar metastasis in sagittal FSE T1 (white arrow) from unknown primary tumor. (B) The primary tumor detection and staging study on coronal multiplanar reconstruction image with gray scale diffusion contrast inversion of the whole body shows the primary detection of prostate neoplasia (thick arrow in A), bone metastases of the spine (arrowheads), right pelvis (short arrow) and multiple lymphadenopathy at the retroperitoneal and thoracic level (long arrows). (C) Control coronal MR image of multiplanar reconstruction with contrast inversion in gray scale in whole-body diffusion at 4 months after treatment with hormonal blockade and radiotherapy demonstrates absence of lesions, in relation to complete response. (D) Sagittal FSE T1 image in the initial study showing involvement of D4 and L3 (arrows). (E) Sagittal in FSE T1 at 4 months post-treatment in radiotherapy and hormonal blockade shows morphological stability (arrows), while diffusion (C) allows assessing the complete response due to the absence of diffusion restriction (resolution of the lesions in B, arrowheads), in correlation with the clinical response of PSA decrease. The solely morphological criterion would have incorrectly interpreted the therapeutic response. FSE, fast spin echo; MR, magnetic resonance; PSA, prostate-specific antigen.

Conclusions

MRI is the technique of choice in the evaluation of bone marrow pathology. For its correct interpretation, it is necessary an optimal knowledge of the different morphological and functional sequences; in order to provide effective diagnoses and to differentiate physiological processes from pathological processes. MRI is able to differentiate physiological changes in the bone marrow between conversion and reconversion, between red and yellow marrow, based on the signal changes of the different sequences; and pathological processes of infiltration, proliferation or vascularization of the physiological ones.

The usefulness of MRI is at any stage of pathological processes; from detection, characterization, staging and monitoring therapy.

Acknowledgments

Funding: None.

Footnote

Provenance and Peer Review: With the arrangement by the Guest Editors and the editorial office, this article has been reviewed by external peers.

Conflicts of Interest: All authors have completed the ICMJE uniform disclosure form (available at https://qims.amegroups.com/article/view/10.21037/qims-23-1678/coif). The special issue "Advances in Diagnostic Musculoskeletal Imaging and Image-guided Therapy" was commissioned by the editorial office without any funding or sponsorship. T.M.N. is an employee of HT Medica. The authors have no other conflicts of interest to declare.

Ethical Statement: The authors are accountable for all aspects of the work in ensuring that questions related to the accuracy or integrity of any part of the work are appropriately investigated and resolved.

References

1. Lin S, Ouyang T, Kanekar S. Imaging of Bone Marrow. Hematol Oncol Clin North Am 2016;30:945-71.
2. Tyler PA, Rajakulasingam R, Saifuddin A. Normal Bone Marrow and Non-neoplastic Systemic Hematopoietic Disorders in the Adult. Semin Musculoskelet Radiol 2023;27:30-44.
3. Mourad C, Cosentino A, Nicod Lalonde M, Omoumi P. Advances in Bone Marrow Imaging: Strengths and Limitations from a Clinical Perspective. Semin Musculoskelet Radiol 2023;27:3-21.
4. Murphy DT, Moynagh MR, Eustace SJ, Kavanagh EC. Bone marrow. Magn Reson Imaging Clin N Am 2010;18:727-35.
5. Shah LM, Hanrahan CJ. MRI of spinal bone marrow: part I, techniques and normal age-related appearances. AJR Am J Roentgenol 2011;197:1298-308.
6. Hanrahan CJ, Shah LM. MRI of spinal bone marrow: part 2, T1-weighted imaging-based differential diagnosis. AJR Am J Roentgenol 2011;197:1309-21.
7. Arrigoni F, Bruno F, Zugaro L, Natella R, Cappabianca S, Russo U, Papapietro VR, Splendiani A, Di Cesare E, Masciocchi C, Barile A. Developments in the management of bone metastases with interventional radiology. Acta Biomed 2018;89:166-74.
8. Mattera M, Reginelli A, Bartollino S, Russo C, Barile A, Albano D, Mauri G, Messina C, Cappabianca S, Guglielmi G. Imaging of metabolic bone disease. Acta Biomed 2018;89:197-207.
9. Vanel D, Casadei R, Alberghini M, Razgallah M, Busacca M, Albisinni U. MR imaging of bone metastases and choice of sequence: spin echo, in-phase gradient echo, diffusion, and contrast medium. Semin Musculoskelet Radiol 2009;13:97-103.
10. Schweitzer ME, Levine C, Mitchell DG, Gannon FH, Gomella LG. Bull's-eyes and halos: useful MR discriminators of osseous metastases. Radiology 1993;188:249-52.
11. Padhani AR, van Ree K, Collins DJ, D'Sa S, Makris A. Assessing the relation between bone marrow signal intensity and apparent diffusion coefficient in diffusion-weighted MRI. AJR Am J Roentgenol 2013;200:163-70.
12. Chan BY, Gill KG, Rebsamen SL, Nguyen JC. MR Imaging of Pediatric Bone Marrow. Radiographics 2016;36:1911-30.
13. van Vucht N, Santiago R, Lottmann B, Pressney I, Harder D, Sheikh A, Saifuddin A. The Dixon technique for MRI of the bone marrow. Skeletal Radiol 2019;48:1861-74.
14. Vilanova JC, Baleato-Gonzalez S, Romero MJ, Carrascoso-Arranz J, Luna A. Assessment of Musculoskeletal Malignancies with Functional MR Imaging. Magn Reson Imaging Clin N Am 2016;24:239-59.
15. Del Grande F, Farahani SJ, Carrino JA, Chhabra A. Bone marrow lesions: A systematic diagnostic approach. Indian J Radiol Imaging 2014;24:279-87.
16. Howe BM, Johnson GB, Wenger DE. Current concepts in MRI of focal and diffuse malignancy of bone marrow.

Semin Musculoskelet Radiol 2013;17:137-44.
17. Vilanova JC, Luna A. Bone marrow invasion in multiple myeloma and metastatic disease. Radiologia 2016;58 Suppl 1:81-93.
18. Isaac A, Dalili D, Dalili D, Weber MA. State-of-the-art imaging for diagnosis of metastatic bone disease. Radiologe 2020;60:1-16.
19. Suva LJ, Washam C, Nicholas RW, Griffin RJ. Bone metastasis: mechanisms and therapeutic opportunities. Nat Rev Endocrinol 2011;7:208-18.
20. Migliorini F, Maffulli N, Trivellas A, Eschweiler J, Tingart M, Driessen A. Bone metastases: a comprehensive review of the literature. Mol Biol Rep 2020;47:6337-45.
21. Guise TA, Mohammad KS, Clines G, Stebbins EG, Wong DH, Higgins LS, Vessella R, Corey E, Padalecki S, Suva L, Chirgwin JM. Basic mechanisms responsible for osteolytic and osteoblastic bone metastases. Clin Cancer Res 2006;12:6213s-6s.
22. Balliu E, Vilanova JC, Peláez I, Puig J, Remollo S, Barceló C, Barceló J, Pedraza S. Diagnostic value of apparent diffusion coefficients to differentiate benign from malignant vertebral bone marrow lesions. Eur J Radiol 2009;69:560-6.
23. Dimopoulos MA, Moreau P, Terpos E, Mateos MV, Zweegman S, Cook G, Delforge M, Hájek R, Schjesvold F, Cavo M, Goldschmidt H, Facon T, Einsele H, Boccadoro M, San-Miguel J, Sonneveld P, Mey U; ESMO Guidelines Committee. Electronic address: clinicalguidelines@esmo. Multiple myeloma: EHA-ESMO Clinical Practice Guidelines for diagnosis, treatment and follow-up(†). Ann Oncol 2021;32:309-22.
24. Hillengass J, Usmani S, Rajkumar SV, Durie BGM, Mateos MV, Lonial S, et al. International myeloma working group consensus recommendations on imaging in monoclonal plasma cell disorders. Lancet Oncol 2019;20:e302-12.
25. Messiou C, Hillengass J, Delorme S, Lecouvet FE, Moulopoulos LA, Collins DJ, Blackledge MD, Abildgaard N, Østergaard B, Schlemmer HP, Landgren O, Asmussen JT, Kaiser MF, Padhani A. Guidelines for Acquisition, Interpretation, and Reporting of Whole-Body MRI in Myeloma: Myeloma Response Assessment and Diagnosis System (MY-RADS). Radiology 2019;291:5-13.
26. Vande Berg BC, Kirchgesner T, Acid S, Malghem J, Vekemans MC, Lecouvet FE. Diffuse vertebral marrow changes at MRI: Multiple myeloma or normal? Skeletal Radiol 2022;51:89-99.
27. Bao H, He X, Li X, Cao Y, Zhang N. Magnetic resonance imaging study of normal cranial bone marrow conversion at high altitude. Quant Imaging Med Surg 2022;12:3126-37.
28. Lin TT, Hu CC, Hsu YC, Wang CC, Chiang SW, Wang CY, Chang WC, Huang GS. Utility of magnetic resonance spectroscopy and diffusion-weighted imaging for detecting changes in the femoral head in divers with hip pain at risk for dysbaric osteonecrosis. Quant Imaging Med Surg 2022;12:43-52.
29. Lecouvet FE, Larbi A, Pasoglou V, Omoumi P, Tombal B, Michoux N, Malghem J, Lhommel R, Vande Berg BC. MRI for response assessment in metastatic bone disease. Eur Radiol 2013;23:1986-97.
30. Padhani AR, Lecouvet FE, Tunariu N, Koh DM, De Keyzer F, Collins DJ, Sala E, Schlemmer HP, Petralia G, Vargas HA, Fanti S, Tombal HB, de Bono J. METastasis Reporting and Data System for Prostate Cancer: Practical Guidelines for Acquisition, Interpretation, and Reporting of Whole-body Magnetic Resonance Imaging-based Evaluations of Multiorgan Involvement in Advanced Prostate Cancer. Eur Urol 2017;71:81-92.
31. Roca-Espiau M, Valero-Tena E, Ereño-Ealo MJ, Giraldo P. Structured bone marrow report as an assessment tool in patients with hematopoietic disorders. Quant Imaging Med Surg 2022;12:3717-24.

Cite this article as: Vilanova C, Martín-Noguerol T, García-Figueiras R, Baleato-González S, Vilanova JC. Bone marrow magnetic resonance imaging (MRI): morphological and functional features from reconversion to infiltration. Quant Imaging Med Surg 2024. doi: 10.21037/qims-23-1678